2D Ising Model

– Computational Physics Assignment 2 –

Lukas Welzel

Faculty of Science, Leiden University
e-mail: welzel@strw.leidenuniv.nl

March 28, 2023

Context. Simulating complex material properties has enabled the design of energy efficient and safe products. The Ising model can be used to predict the ferromagnetic properties of lattices.
Aims. We will simulate a 2D lattice of interacting spins in order to find spontaneous magnetization regions and phase transitions.
Methods. We use a Monte Carlo method, the Metropolis algorithm to find and observe the equilibrium state of a 2D lattice..
Conclusions. We find emergent ferromagnetic behaviour as well as phase transitions for the 2D lattice. Furthermore, we comment on the spin correlation function and propose a novel potential solution to the problem of spin auto-correlation for small lattices with large spin-interaction kernels.
Key words. Ising model – numerical methods – magnetism

Contents

1 Introduction 1
2 Methods 1
3 Results 2
4 Discussion 4
5 Conclusion 7

1. Introduction

The Ising model is probably one of the most studied problem in statistical physics. its applications range from neuroscience to computational materials design. We use Monte Carlo methods on the Ising model to investigate the ferromagnetic behaviour of 2D lattices of interacting spins.

2. Methods

2.1. Model

The two dimensional Ising model over a $N \times N$ square lattice $\mathcal{L}$ is described by the Hamiltonian

$$\mathcal{H} = J_1 \sum_{nn} s_i s_j + J_2 \sum_{nnn} s_i s_k + J_3 - H \sum_i s_i, \tag{1}$$

where J_i are the coupling constants, in this work all $J = 1$, $s \in [-1, 1]$ are the spins of the cells which interact with their nearest neighbours (nn) or next nearest neighbours (nnn) and H is an external magnetic field, which we set to zero in this work. In this work we use a Metropolis algorithm, a class of Monte Carlo algorithms which are based on Markov processes, to investigate the system at equilibrium. This means that we require our system and method to be ergodic, i.e. our method should be able to reach any state of the system from any other. Furthermore, we require that our system is in detailed balance, so that the transition probabilities $T(x \to x')$ of moving from state x to x' do not only fulfil Equation 2, but the stronger requirement Equation 3.

$$\sum_{x'} T(x \to x') = 1 \tag{2}$$

Hence, we require the probabilities of transferring from state x to x' to be in detailed balance.

$$p(x, i) T(x \to x') = p(x', i) T(x' \to x) \quad \forall x, x', \tag{3}$$

where at time i the probability p of state x, is only dependent on the probabilities of the system at $i - 1$. In this work we work with discrete time, so i will be a discrete step. Since the probabilities need to be sampled from a Boltzmann distribution we write Equation 4, which means that probability $A_{xx'}$ of accepting a state x' from state x must be given by Equation 5 to fulfill the detailed balance, i.e. be symmetric.

$$\frac{p_x}{p_{x'}} = \frac{\frac{1}{Z} e^{-\beta E_x}}{\frac{1}{Z} e^{-\beta E_{x'}}} = e^{-\beta \Delta E}, \tag{4}$$

where the energy difference of the system at the two states is $\Delta E = \mathcal{H}(x') - \mathcal{H}(x)$, and the system is at temperature $T = 1/(\beta k_B)$, with k_B the Boltzmann constant and β the inverse temperature.

$$A_{xx'} = \begin{cases} 1 & \text{if } p(x') > p(x) \\ p(x')/p(x) & \text{if } p(x') < p(x) \end{cases} \tag{5}$$

We solve this equation while propagating the system. This propagation does not mean mean moving forwards in time but rather towards system equilibrium in its thermal bath. To do this we test flipping a spin and evaluating the change in energy of the system, and through that the probability of accepting this new state. To ascertain that the system has sufficient time to evolve in between measurements i.e. we fulfill ergodicity, we measure in steps of $N \times N$ interactions and hence do a quasi-sweep of the system since the spin site selection is random. At any temperature $T \neq 0$, the system reaches its equilibrium state after sufficient interactions, independent of its initial conditions. Hence,

we can estimate the system properties, and their posteriors, using the Monte Carlo integration scheme in Equation 6.

$$\int A(x)p(x)dx \approx \frac{1}{N}\sum_{i=1}^{N} A(x_i) \tag{6}$$

2.2. Computational Method

We implement above method in python using `numpy`, `numba` and `statsmodels` which we use to estimate the auto-correlation time of the system. Firstly we initialize a $N \times N$ system with a potentially biased initial state towards. Again, the system tends towards its equilibrium state regardless of the initial bias. Secondly, we initialize a kernel $\mathcal{K}$ which defines the (n)-nearest neighbours via their distance to a site. The kernel shape is defined by the kernel radius r_k and includes neighbours for which $r_k \geq r$, where r is the euclidean distance between site and neighbour. The interaction strength is weighted by their inverse distance squared and normalizing by the total interaction strength so that the total weight is 4 for all setups, see Equation 7.

$$\mathcal{K}_{i,j} \propto \frac{1}{r_{i,j}^2}, \quad \text{with} \quad 4 = \sum \mathcal{K} \tag{7}$$

Nevertheless, in the following we do not investigate the impact of varying the neighbour interaction strength weighting.[1] Assigning different weights leads to frustration fields due to the formation of structure (e.g. Néel, superantiferromagnetic or quadruple, depending on the ratio of $J_{1,2,3}$ and the size of the kernel). (Kassan-Ogly et al. 2015) Furthermore, we rescale the temperature according to the kernel, see Equation 8, with respect to the nearest neighbours model.

$$T'(r_k) = T(r_k = 1)\frac{\sum\lceil\mathcal{K}(r_k)\rceil_{[0\vee1]}}{\sum\lceil\mathcal{K}(r_k = 1)\rceil_{[0\vee1]}}, \tag{8}$$

where $\sum\lceil\mathcal{K}(r_k)\rceil_{[0\vee1]}$ are the unweighted, not normalized stencils, which in the code are boolean kernels implicitly cast to floats. We impose periodic boundary conditions by allowing the kernel to wrap over the boundaries of the lattice. Thirdly, we measure the total energy of the system using Equation 1 by multiplying its inverse with the convolution of the lattice with the interaction kernel, summing the site energies and renormalizing to avoid the double counting of pairs, see Equation 9.

$$\mathcal{H} = -\frac{1}{2}\sum \mathcal{L} \cdot [\mathcal{L} * \mathcal{K}] \tag{9}$$

This is a computationally much more efficient way to find the total energy of the lattice, compared to Equation 1. Fourthly, we let the system relax into its equilibrium state. The relaxation time, as well as the auto-correlation time of the system, is strongly dependent on the system temperature according to Stoll et al. (1973), hence we allow systems to dynamically adjust their relaxation time. As a criterion for the relaxation time we choose the mean absolute spin $\langle|m|\rangle$ of the system. If a system is relaxed, there are two options:

1. The system is (super)antiferromagnetic and the mean absolute spin, measure over sufficient steps is close to zero.
2. The system is ferromagnetic and the mean absolute spin, measure over sufficient steps is close to one.
3. The system is near its critical point and the mean spin switches between minus and plus one, since the transition time between the metastable states is short compared to their half-live, this is approximated equivalent to option two over a sufficiently long time. This is also true for lattices with different interactions ratios.[2]

The previously defined kernel acts as a stencil on the lattice, which determines the interacting sites. We randomly select a site for testing a spin flip and evaluate the consequences, i.e. the change in energy, evaluated under the stencil. We then either accept or reject the change according to Equation 5. After sweeping over $N \times N$ random sites we measure the system properties; magnetization and energy and progress to the next sweep. Fifthly, when the system is relaxed, we measure its auto-correlation time τ. We implement an auto-correlation time estimator approximating Equation 10.

$$\int_0^\infty \frac{\chi(t)}{\chi(0)} = \int_0^\infty e^{-t/\tau}dt = \tau, \tag{10}$$

where $\chi(t)$ is the discrete auto-correlation function given in Equation 11.

$$\begin{aligned}\chi(t) =& \frac{1}{t_{\max} - t}\sum_{t'=0}^{t_{\max}-t} m(t')\,m(t'+t) \\ &- \frac{1}{t_{\max} - t}\sum_{t'=0}^{t_{\max}-t} m(t') \times \frac{1}{t_{\max} - t}\sum_{t'=0}^{t_{\max}-t} m(t'+t),\end{aligned} \tag{11}$$

where m is a (time) series and t_{max} is the final time (discrete timestep) of the series. However, using Equation 11 is computationally inefficient compared to utilizing fast Fourier transform (FFT) to compute the discrete Fourier transform of the time-series. Both methods estimate the self similarity of the signal as a function of its self-lag, and are hence both suited for estimating τ. Nevertheless, both lag behind more sophisticated methods since they require a long time series compared to the auto-correlation time to reliably estimate τ. The corresponding requirement on our method is that $t_{max} \gg \tau$. We additionally impose a 95% confidence requirement for estimating the correct auto-correlation time. We then move on towards measuring the properties of the system by observing it for 100 or 1000 blocks of 16 auto-correlation times, depending on available resources and/or assumed auto-correlation time. Both should be sufficient for enough independent measurements.

3. Results

In this work we observe a numerical 2D Ising model on a 50×50 site lattice in a square configuration. We observe the model at a range of dimensionless temperature, from 1 to 4, evaluated at intervals of 0.2 and 0.1, where we perform roughly 18 independent measurements for each observation at 0.2 steps. Additionally, we evaluate the 2D model at its critical temperature T_c, see Equation 12, which has been evaluated analytically by e.g. Onsager (1944).

$$\frac{k_B T_c}{J} = \frac{2}{\ln(1+\sqrt{2})} \approx 2.269 \tag{12}$$

[1] Mainly due to the computational effort increasing quickly when the graph becomes more connected by including more nearest neighbours.

[2] Note how this is different from the mean absolute magnetization shown in Figure 1 near the critical point due to the measurement times.

We investigate different (n)-nearest neighbour models similarly, with fewer independent measurements and rescaled interaction parameters according to section 2.

We estimate the standard deviation of the magnetic susceptibility and specific heat per spin using Equation 13 in order to break auto-correlation effects for chains with $t_{\max} \gg \boldsymbol{\tau}$.

$$\sigma_m^2 = \frac{2\tau}{t_{\max}} \left(\left\langle m^2 \right\rangle - \langle m \rangle^2 \right), \tag{13}$$

where m is the sampled variable. (Glauber 1963)

3.1. Auto-Correlation Time

We evaluate the auto-correlation time according to Equation 10. The plot for $k_r = 1$ is shown in Figure 1 and implies stability in both ferro- or antiferromagnetic regions, compare Figure 2, and instability near the critical temperature. Note that in our model

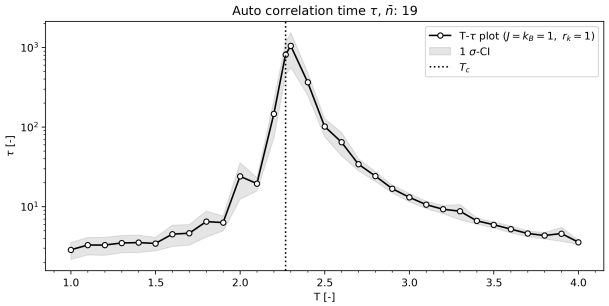

Fig. 1: Auto-correlation time as a function of temperature. The auto-correlation time is large when the system is near its critical temperature, and the uncertainty associated with these measurements is also large. The auto-correlation time for both high and low mean absolute magnetization is very low which indicates stability even on small timescales (small lag of a few sweeps), whereas high auto-correlation time implies the opposite near the critical point. Note the log_{10}-scale.

the the auto-correlation time at the critical temperature is not infinite nor undefined.

3.2. Magnetization

The mean absolute magnetization $\langle |m| \rangle$ is given in Equation 14 and shown for $k_r = 1$ in Figure 2. Over the temperature sweep a phase transition is clearly visible. At low temperatures the lattice is highly magnetized with aligned spins which are strongly coupled (their spin at $i+1$ is highly correlated with their neighbours spin at i), whereas at high temperature the spins are essentially independent, especially for sites which are not neighbours.

$$\langle |m| \rangle = \frac{1}{N^2} \left\langle \left| \sum_i s_i \right| \right\rangle \tag{14}$$

The impact of the instability mentioned above is visible in the relatively larger confidence interval near the critical point. Still, the magnetization closely follows a sharp logistic function, which approximates binary discrete distribution, i.e. indicates a phase transition near the critical point. Importantly, the magnetization as $\lim_{T \to \infty}$ does not approach zero and some magnetization remains.

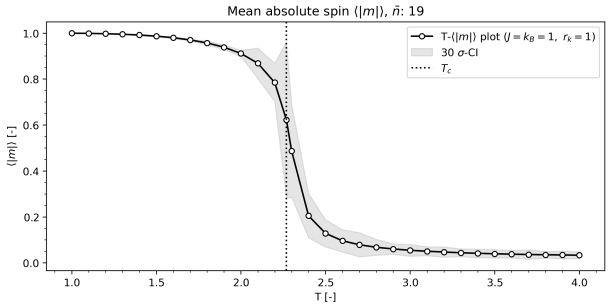

Fig. 2: Mean absolute magnetization as a function of temperature. The curve indicates a phase transition near the critical temperature.

3.3. Energy

The mean energy e is given in Equation 15 and shown for $k_r = 1$ in Figure 3. Its behaviour behaviors is similar to the magnetization since both are closely related through the sum of spins. The equilibrium energy is higher for lattices at higher temperatures.

$$e = \left\langle \frac{E}{N^2} \right\rangle \tag{15}$$

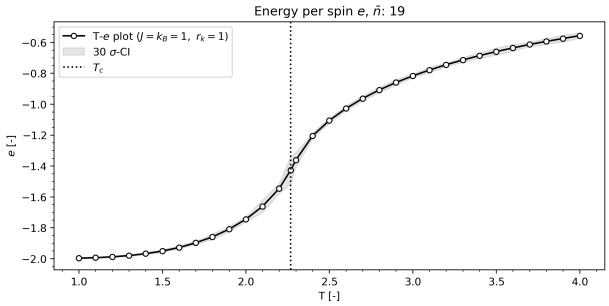

Fig. 3: Mean energy as a function of temperature. The curve indicates, unsurprisingly, that systems with lower temperature are at lower energies, but also that a phase transition is near the critical temperature.

3.4. Magnetic Susceptibility

The magnetic susceptibility χ_M, Equation 16, again shows a phase transition, see Figure 4. The larger the lattice becomes the more pronounced the peak of the distribution, and the close the peak gets to the critical temperature from the analytic solution. I am not sure why the standard deviation is so weird here, especially why it is so small near the critical point. I think it is because of the long chain length impacting the estimator in Equation 13.

$$\chi_M = \frac{\beta}{N^2} \frac{\partial \langle M \rangle}{\partial H} = \frac{\beta}{N^2} \left(\left\langle M^2 \right\rangle - \langle M \rangle^2 \right) \tag{16}$$

3.5. Specific Heat

The specific heat per spin C, Equation 17, behaves similar to the magnetic susceptibility, in so far that the sharpness of the

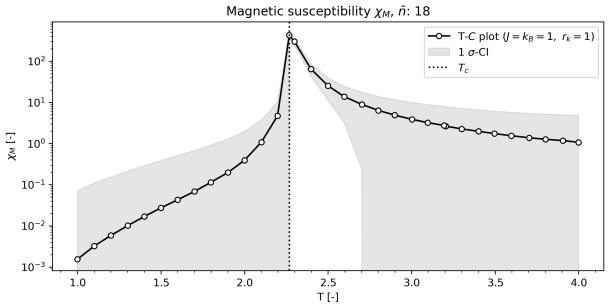

Fig. 4: Magnetic susceptibility plotted against temperature. A phase transition is visible near the critical temperature.

transition also depends on the the lattice size, see subsection 4.4.

$$C = \frac{\partial E}{\partial T} = \frac{1}{N^2 k_B T^2} \frac{\partial^2 \ln Z}{\partial \beta^2} = \frac{1}{N^2 k_B T^2} \left(\left\langle E^2 \right\rangle - \langle E \rangle^2 \right), \quad (17)$$

where Z is the partition function. The heat capacity is shown in Figure 5.

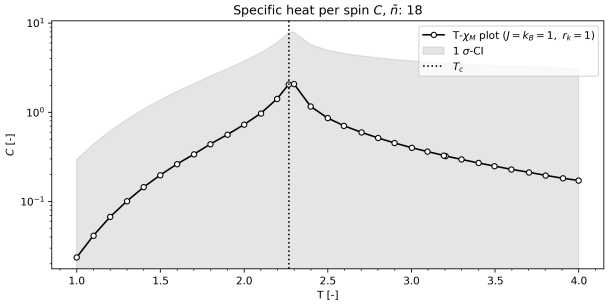

Fig. 5: The specific heat per spin as a function of temperature. The phase transition near the critical temperature is visible, however not as pronounced as for the magnetic susceptibility.

3.6. Interaction Kernel

In Figure 6 and Figure 7 the above plots are show for a kernel with $k_r = 2$ and $k_r = 3$ respectively. We did not observe the system for more square kernels, instead focusing on multiples of the lattices smallest periodicity.

4. Discussion

4.1. Auto-Correlation Time

As highlighted, the auto-correlation time at the critical temperature is not infinite, at least to the accuracy of the model. This implies that either there is some natural stability to the magnetization of the lattice at the meta-stable critical point. We expect that the auto-correlation time at that temperature is the periodicity of the meta-stability, since the magnitude of correlation with a lagged signal would be dominated by the magnetization change, and hence the FFT would find the auto-correlation time only on that time scale with the required confidence when lagging the signal. However, the way in which we determine the auto-correlation time during the relaxation is limited by the maximum number of sweeps we allow. The primitive methods we use in this work to find τ estimate an auto-correlation time some times larger than the total signal time, see e.g. Kissling and Carl (2008); F. Dormann et al. (2007) and Bos et al. (2002) for a comparison. For the lattices in Figure 1 the maximum number of relaxation sweeps was 10^3. Based on evaluating the auto-correlation time for the entire observation, increasing the maximum number of relaxations weeps and the the magnetization time series for models near the temperature I suspect that instead of detecting the actual auto-correlation time we detect the limit of our algorithm. Implementing and training an auto-regressive model is not feasible in the available time. Based on the discussion above and the similarity the Ising model has to chaotic bi-stable systems (see King and Gaito (1992); Nekorkin and Makarov (1995), and more directly related Heugel et al. (2021)) I suspect that the auto-correlation time is technically undefined for an arbitrarily large or correlation breaking numerical 2D Ising model, i.e. diverges at the critical temperature, and we just impose/wrongly estimate the auto-correlation at $\tau > t_{max}$ with the maximum time.[3] (Stoll et al. 1973)

4.2. Magnetization

The emergent (spontaneous, at low temperatures) magnetization of the lattice stems from the coupling strength between neighbours which is a function of the temperature, see Equation 4. As the stencil around each site is much smaller than the total lattice, if the correlation moment between (n) nearest neighbours $\rho_{x,x'} \propto e^{-\beta} = \varepsilon$, the (n) l^{th}-removed neighbours are correlated as $\varepsilon^l \leq \rho_{x,x^l} \leq \sum_l \sum \lceil \mathcal{K}(r_k) \rceil_{[0 \vee 1]}^l \varepsilon^l$, since multiple paths can exist for interactions. (Aizenman and Lebowitz 1988) Hence, for large temperatures even for close sites the probabilities are essentially uncorrelated. (Diep et al. 2013) Analogously, the inverse is the case for low temperatures where the the spins are highly correlated so that the probability of a sufficient number (Peierls droplet) of spins to flip is small. In real lattices the analysis is complicated by their often large size, discontinuities and non square lattice, which allows the formation and stability of superselection sectors. (Kitaev 2006; Diep et al. 2013)

The apparent position of the phase transition is not only a function of the critical temperature, instead it depends at least also on the lattice size. When performing test for smaller lattices we found that for smaller lattice sizes the apparent position of the phase transition shifts towards lower temperatures so that the model lattice needs to be infinite for the critical temperature to coincide with the analytic solution.

4.3. Energy

From the analytic solution we expect a discontinuity in the first derivative of the energy at (near) the critical temperature. In our model we do not detect this discontinuity. I do not think we could detect the discontinuity in a reasonable time with our resolution and variance.

4.4. Magnetic Susceptibility

I suspect the asymmetry in the auto-correlation time, magnetization and energy is due to the finite size of the lattice. When running other lattice sizes, especially the magnetic susceptibility

[3] The arguments about the auto-correlation time in 3 dimensions are so highly cursed. Schrader (1976): "simple proof", very funny.

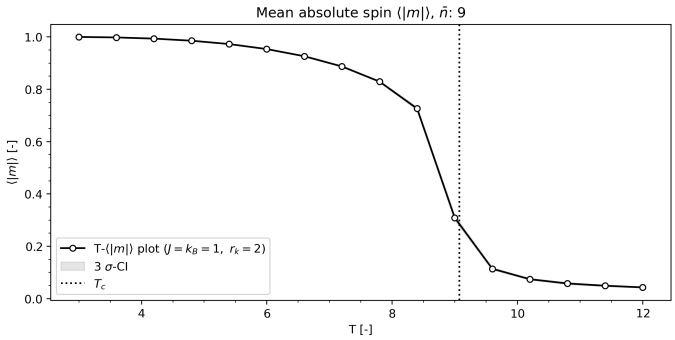

(a) Mean absolute magnetization as function of temperature.

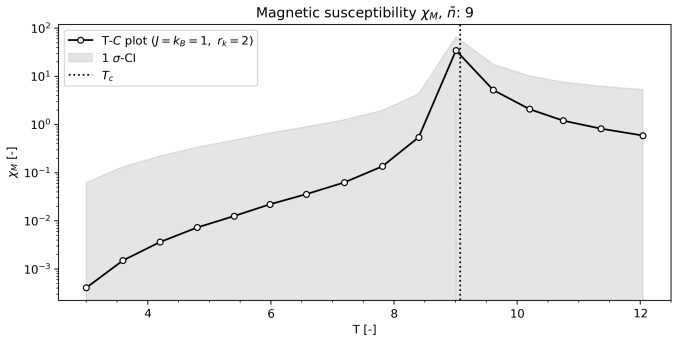

(b) Magnetic susceptibility as function of temperature.

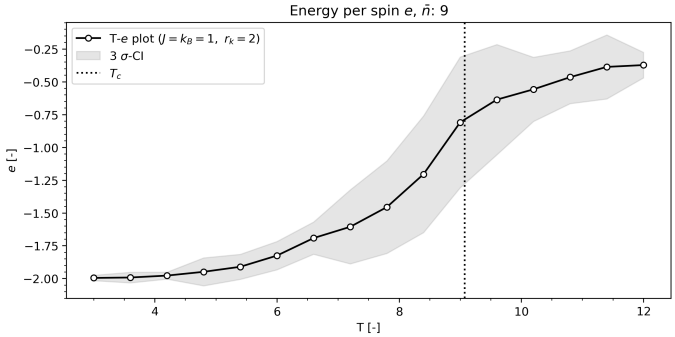

(c) Mean energy as function of temperature.

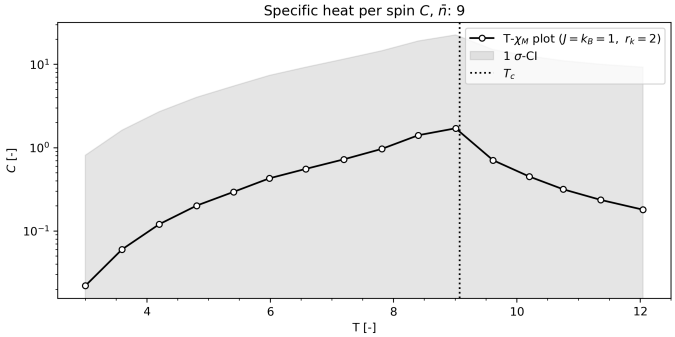

(d) Specific heat per spin as function of temperature.

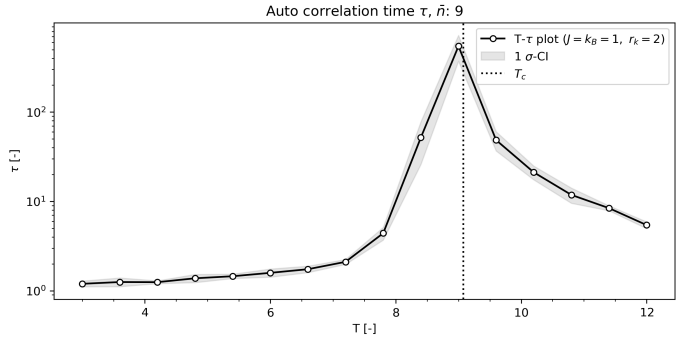

(e) Auto-correlation time as function of temperature.

Fig. 6: Temperature sweep plots for the Ising model with a interaction kernel of radius $k_r = 2$. The overall shape of the plots is equivalent as for the $\mathcal{K}(k_r = 1)$ kernel, for properly rescaled variables. The phase transition is again clear, however at a larger temperature since each sites "binding" energy is higher, i.e. each site affects a relatively larger part of the lattice.

approaches the critical temperature for larger ones, so that:

$$\frac{C_{crit}}{kN^2} \propto \ln N, \tag{18}$$

And we infer that for real systems with much larger lattices the heat capacity at the critical temperature is practically a discontinuity. (Kryzhanovsky et al. 2018) I think this is due to the limited number of paths that are available for interactions, so that the sites are actually more strongly correlated, than they should be for even larger or infinite lattices. This is partially due to the image convention that we chose which wraps the lattice around and hence does not break correlation at the boundaries. I am not sure if it is possible to analytically impose a randomly distributed boundary condition from the quasi-1D Ising model there, depending on the spins on the boundaries to break this extra correlation.

As mentioned in subsection 4.3, we do not detect a discontinuity in the first derivative of the lattice energy, however, such a discontinuity should also result in a drop in the heat capacity near the critical temperature, as we increase the temperature beyond the discontinuity in energy. While the resolution of our sweep is not sufficient to position this drop, it is noteworthy that the asymmetry of the heat capacity around the critical temperature is not the same as for the other variables, which could be an indicator for this drop in C. From this tenuous indicator we also infer that the phase transition at T_c is second-order, since the energy is continuous, and its first derivative is discontinuous. Nevertheless, literature also suggest the existence of a first-order transition, see e.g. Isakov (1984), compare with Dotsenko and Dotsenko (1983), as $\lim_{H\to 0}$.[4] Since our model is at $H = 0$, this is not necessarily directly transferable due to the discontinuous analysis near T_c. (Isakov 1984)

[4] The analytic solutions for the mean field model do some heavy lifting here though.

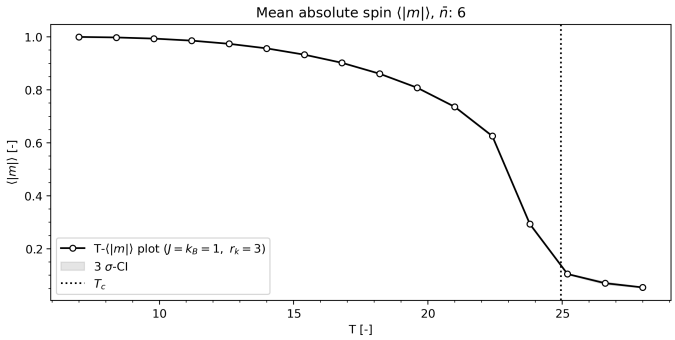

(a) Mean absolute magnetization as function of temperature.

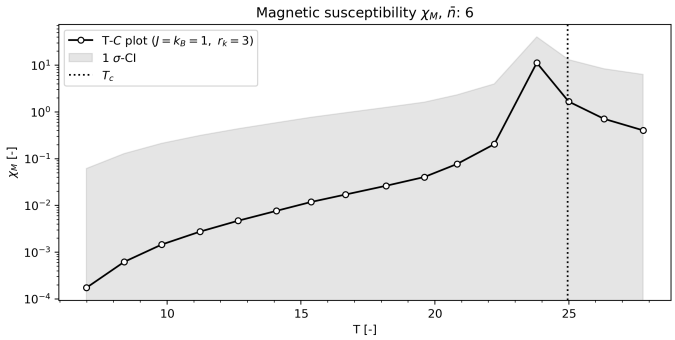

(b) Magnetic susceptibility as function of temperature.

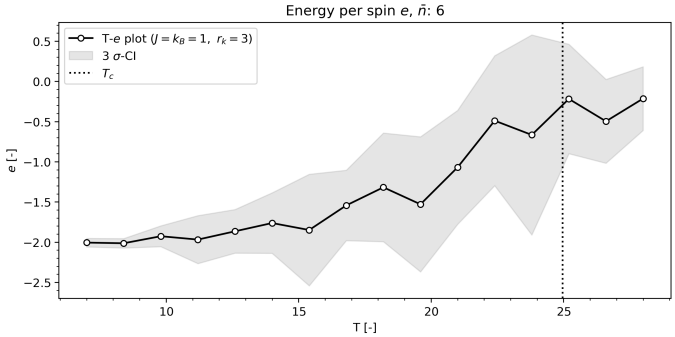

(c) Mean energy as function of temperature.

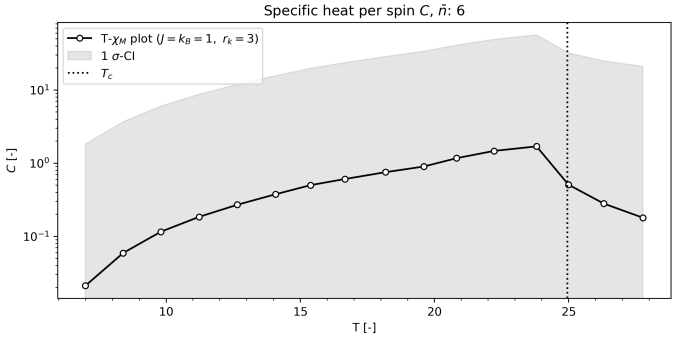

(d) Specific heat per spin as function of temperature.

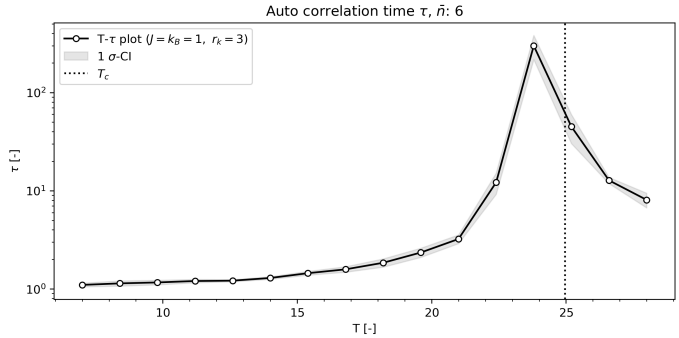

(e) Auto-correlation time as function of temperature.

Fig. 7: Temperature sweep plots for the Ising model with a interaction kernel of radius $k_r = 3$. The overall shape of the plots is equivalent as for the $\mathcal{K}(k_r = 1)$ kernel, for properly rescaled variables. The phase transition is again clear, however at a larger temperature since each sites "binding" energy is higher, i.e. each site affects a relatively larger part of the lattice. For this kernel the lattice starts to become too small since interactions can auto-correlate within a few timesteps/sweeps. This is shown by the the phase transition occuring significantly below the critical temperature.

4.5. Interaction Kernel

The interaction kernel size does not affect the general and overall properties of the system, however choosing specific relative interaction strengths can lead to structure forming such as discussed by Kassan-Ogly et al. (2015) which we can anecdotally replicate. Nevertheless, we find that having the interaction strength scale with distance makes initiative sense, considering spin-spin and electron-electron interactions. (Wu et al. 1976; Delfino and Mussardo 1995) However, there are clearly cases where we can imagine a modulated spin-spin correlation functions, e.g. conducting lattices, grain boundaries, impurities or strained lattices with Type II Strained-Layer Superlattices as a specific example. (McCoy and Wu 1969; Merz and Chalker 2002)

Nevertheless, in our investigation we have two important findings, firstly, our use of stencil based nearest neighbour determination means that propagating the Ising model with larger kernels did not significantly affect runtime, secondly, for kernels that become large there mus be an external auto-correlation breaking mechanism to preserve the behaviour of the system. We propose the use of a buffer, i.e. a stack of past transitions, from which can be randomly dawn to break correlations for these relatively small lattices. This buffer opens up two possibilities, the use of the buffer to purposefully explore new regions of the state space through prioritizing these unknown transitions, notably without violating ergodicity, and a build-in method for dynamically estimating auto-correlation time via FFT. To my knowledge this is a novel idea.[5] Interesting would also be the application of deep reinforcement learning methods to learn the behaviour of Ising models for computational material design, com-

[5] If its good is completely different question though.

pare e.g. Imanaka et al. (2021); Angermueller et al. (2019); Wu et al. (2019).

5. Conclusion

In this work we develop a fast 2D numerical Ising model to investigate the behaviour of lattices with interacting spins at discrete sites. We find that the lattices undergo a phase transition at a critical temperature. Our numerical methods can approximately identify the location the phase transition and in the limit of an infinite lattice we infer agreement with the analytic solution. We implement different spin correlation functions and investigate how they change the model. We find that, for inverse squared distance weighted spin-spin correlations the behaviour is similar to the nearest neighbours only kernel. We find a problem with the 2D Ising model when kernel and lattice size become relatively similar due to auto-correlation on the order of some steps. We propose a novel method for breaking this correlation based on drawing random past transitions from a buffer.

References

Aizenman, M. and Lebowitz, J. L. (1988). Metastability effects in bootstrap percolation. *Journal of Physics A: Mathematical and General*, 21(19):3801.

Angermueller, C., Dohan, D., Belanger, D., Deshpande, R., Murphy, K., and Colwell, L. (2019). Model-based reinforcement learning for biological sequence design. In *International conference on learning representations*.

Bos, R., De Waele, S., and Broersen, P. M. (2002). Autoregressive spectral estimation by application of the burg algorithm to irregularly sampled data. *IEEE Transactions on Instrumentation and Measurement*, 51(6):1289–1294.

Delfino, G. and Mussardo, G. (1995). The spin-spin correlation function in the two-dimensional ising model in a magnetic field at t= tc. *Nuclear Physics B*, 455(3):724–758.

Diep, H. et al. (2013). *Frustrated spin systems*. World scientific.

Dotsenko, V. S. and Dotsenko, V. S. (1983). Critical behaviour of the phase transition in the 2d ising model with impurities. *Advances in Physics*, 32(2):129–172.

F. Dormann, C., M. McPherson, J., B. Araújo, M., Bivand, R., Bolliger, J., Carl, G., G. Davies, R., Hirzel, A., Jetz, W., Daniel Kissling, W., et al. (2007). Methods to account for spatial autocorrelation in the analysis of species distributional data: a review. *Ecography*, 30(5):609–628.

Glauber, R. J. (1963). Time-dependent statistics of the ising model. *Journal of mathematical physics*, 4(2):294–307.

Heugel, T. L., Zilberberg, O., Marty, C., Chitra, R., and Eichler, A. (2021). Ghost in the ising machine. *arXiv preprint arXiv:2103.02625*.

Imanaka, Y., Anazawa, T., Kumasaka, F., and Jippo, H. (2021). Optimization of the composition in a composite material for microelectronics application using the ising model. *Scientific Reports*, 11(1):1–7.

Isakov, S. (1984). Nonanalytic features of the first order phase transition in the ising model. *Communications in mathematical physics*, 95(4):427–443.

Kassan-Ogly, F., Murtazaev, A., Zhuravlev, A., Ramazanov, M., and Proshkin, A. (2015). Ising model on a square lattice with second-neighbor and third-neighbor interactions. *Journal of Magnetism and Magnetic Materials*, 384:247–254.

King, G. P. and Gaito, S. T. (1992). Bistable chaos. i. unfolding the cusp. *Phys. Rev. A*, 46:3092–3099.

Kissling, W. D. and Carl, G. (2008). Spatial autocorrelation and the selection of simultaneous autoregressive models. *Global Ecology and Biogeography*, 17(1):59–71.

Kitaev, A. (2006). Anyons in an exactly solved model and beyond. *Annals of Physics*, 321(1):2–111.

Kryzhanovsky, B. V., Malsagov, M. Y., and Karandashev, I. M. (2018). Dependence of critical parameters of 2d ising model on lattice size. *Optical Memory and Neural Networks*, 27(1):10–22.

McCoy, B. M. and Wu, T. T. (1969). Theory of a two-dimensional ising model with random impurities. ii. spin correlation functions. *Physical Review*, 188(2):982.

Merz, F. and Chalker, J. (2002). Two-dimensional random-bond ising model, free fermions, and the network model. *Physical Review B*, 65(5):054425.

Nekorkin, V. and Makarov, V. (1995). Spatial chaos in a chain of coupled bistable oscillators. *Physical review letters*, 74(24):4819.

Onsager, L. (1944). Crystal statistics. i. a two-dimensional model with an order-disorder transition. *Physical Review*, 65(3-4):117.

Schrader, R. (1976). New rigorous inequality for critical exponents in the ising model. *Physical Review B*, 14(1):172.

Stoll, E., Binder, K., and Schneider, T. (1973). Monte carlo investigation of dynamic critical phenomena in the two-dimensional kinetic ising model. *Physical Review B*, 8(7):3266.

Wu, D., Wang, L., and Zhang, P. (2019). Solving statistical mechanics using variational autoregressive networks. *Physical review letters*, 122(8):080602.

Wu, T. T., McCoy, B. M., Tracy, C. A., and Barouch, E. (1976). Spin-spin correlation functions for the two-dimensional ising model: Exact theory in the scaling region. *Physical Review B*, 13(1):316.